MONTE CARLO MODEL OF HIGH-VOLTAGE CONDITIONING AND OPERATION

W. L. Millar*, W. Wuensch, CERN, 1211 Geneva 23, Switzerland

G. Burt, Cockcroft Institute, Lancaster University, Lancaster LA1 4YW, UK

Abstract

To synthesise the experimental results and theory pertaining to high-field phenomena, a model has been developed to simulate the conditioning and operation of high-field systems. By using a mesh-based method, the high-field conditioning of any arbitrary geometry and surface electric field distribution may be simulated for both RF and DC devices. Several phenomena observed in previous high-field tests such as the probabilistic behaviour of vacuum arcs and the inhomogeneous distribution of arc locations are described by this approach.

INTRODUCTION

High-voltage conditioning is the progressive increase in an electrode's resistance to arcing which is developed during high-field operation. The process is a relevant topic for any technology where breakdown limits performance and numerous RF and DC test facilities have been established in this context [1–7]. To better understand the results from these facilities and offer insight into how current conditioning procedures could be improved, a new discretised model has been developed.

THE MODEL

The model is based on the progressive modification of the electrode surface and relies on several assumptions. Given the often inhomogeneous field distribution in high-field devices, the electrode geometry divided into individually treated mesh elements. Each element is assigned a scaling factor, k_i, to allow calculation of the local electric field relative to the maximum, E_O, for a given operating voltage. To facilitate inhomogenuous meshing, the number of elements and the area of each, a_i, is also user-definable. Devices may then be simulated with any arbitrary spatial resolution.

Generally, in existing conditioning procedures the field is increased gradually, as the rate at which devices condition quickly decreases when operating at fixed voltages [8–11]. If a constant breakdown rate is maintained during this ramping, the increase in operating field is asymptotic, and this is regularly observed in high-gradient RF cavity tests [8–10]. In one instance, a cavity tested at CERN showed no reduction in the breakdown rate when operated under fixed conditions in the later stages of testing [10]. Results from these, and similar RF cavity tests elsewhere, have also shown that the conditioning of similar devices is most comparable when plotted against the cumulative number of pulses, as opposed to cumulative number of breakdowns [8].

Based on these characteristics, the model assumes a maximum attainable electric field, E_L, for a given reference breakdown rate i.e. probability of arcing, P_{Ref}. The level of conditioning of each element is denoted $E_{S,i}$. In a device with a homogeneous field distribution, E_S then refers to the surface electric field which can be established at the reference breakdown rate. To provide the conditioning effect the model assumes that, in the absence of breakdowns, $E_{S,i}$ is increased with each pulse as:

$$\Delta E_{S,i} = \gamma \cdot \frac{E_O \cdot k_i}{E_{S,i}} \cdot \left[1 - \frac{E_{S,i}}{E_L} \right] \tag{1}$$

where γ is a constant to allow fitting to existing data and has units of V/m. The latter term in Eq. (1) then remains unitless and is scalable for different materials, a characteristic which aligns with existing test results in which different materials were recorded as having conditioned at different rates and to different field levels [12]. In RF cavities, the breakdown rate has been shown to scale with the electric field as [13]:

$$BDR \propto E^{30} \tag{2}$$

However, as conditioning progresses the breakdown rate for a given field level decreases. As such, it is assumed that the probability of breakdown for a given mesh element on each pulse, $P_{BD,i}$, scales with the ratio of the applied electric field to its conditioned state as:

$$P_{BD,i} \propto \left[\frac{E_O \cdot k_i}{E_{S,i}} \right]^{30} \tag{3}$$

Experiments have also shown that it is common for several breakdowns to occur in quick succession, followed by a quiescent period. This has led to the proposal that breakdowns may be classified as primary events, which occur stochastically, and secondary events, which are a consequence of the primary event [8, 9]. It is postulated then, that breakdowns are capable of effectively diminishing the conditioned state the surface. However, as devices are capable of reliably establishing high fields after several breakdowns, improvement is also possible. This could correspond physically, for instance, to the removal of field emission sites capable of nucleating future breakdowns. To capture this effect, a unitless enhancement factor, ψ, is added to Eq. (3) as:

$$P_{BD,i} \propto \left[\frac{E_O \cdot k_i}{E_{S,i} \cdot \psi_i} \right]^{30} \tag{4}$$

_____
* lee.millar@cern.ch

Initially, all the elements' ψ values are assigned randomly from an appropriately tailored Gaussian distribution, as has been used previously to model the evolution of field emission sites during conditioning [14]. If a breakdown is accrued, the element in which it occurred is then assigned a new ψ value. Finally, P_{Ref} is added and the probability is scaled as:

$$P_{BD,i} = a_i \cdot \left[\frac{E_O \cdot k_i}{E_{S,i} \cdot \psi_i} \right]^{30} \cdot \left[1 - \sqrt[G]{1 - P_{Ref}} \right] \quad (5)$$

where G accounts for the field distribution and meshing, and is defined:

$$G = \sum_{i=1}^{n} a_i \cdot k_i^{30} \quad (6)$$

where n is the number of grid elements. In this way, if a given device is fully conditioned and E_O is equal to E_L, the probability of breakdown remains equal to P_{Ref}, irrespective of the meshing and electric field distribution.

RESULTS

RF Cavity Conditioning

Given the availability of data, the model was first applied to the 12 GHz cavities for the CLIC study for tuning and benchmarking [15–17]. However, the framework can in principle be adapted to devices with other operating frequencies and field profiles. Generally, the CLIC cavities are comprised of 24 or 26 tapered accelerating cells and two couplers [17–19]. For simplicity, 24 identical grid elements, each corresponding to a separate accelerating cell, were employed in simulation. As each element is assigned its own enhancement factor, ψ, this approach aligns with experimental data which shows that breakdowns which occur in quick succession often occur spatially close together, or in the same cell [8, 20].

Prototype X-band cavities at CERN and KEK regularly reach accelerating gradients of 100-120 MV/m, corresponding to peak surface electric fields in excess of 200 MV/m [10, 21, 22]. In 2018, a CERN cavity was tested up to a peak surface field of approximately 240 MV/m. While operating at this level, it was noted that the breakdown rate remained fixed at 5×10^{-5} bpp (breakdowns per pulse) and did not decrease [10]. In light of these results, values of 240 MV/m and 5×10^{-5} were selected for E_L and P_{Ref} respectively in simulation. A value of 2 MV/m was chosen for γ and the mean and standard deviation of the Guassian distribution from which the ψ values are selected were set to 1 and 0.12 respectively.

To control the applied field in simulation, the conditioning algorithm from CERN's X-band test stands was imported. In summary, the field level is adjusted to maintain a constant,

operator-selected breakdown rate. Further details of the algorithm are reported elsewhere [1, 23]. In CERN's test stands, conditioning of the protoype CLIC structures generally commences at peak surface electric fields of ≈ 60 MV/m. As such, E_S and E_O were initially set to 60 MV/m in simulation. A breakdown rate setpoint of 3×10^{-5} bpp was selected and the first 200 million pulses of the conditioning process were simulated. The results are shown in Fig. 1.
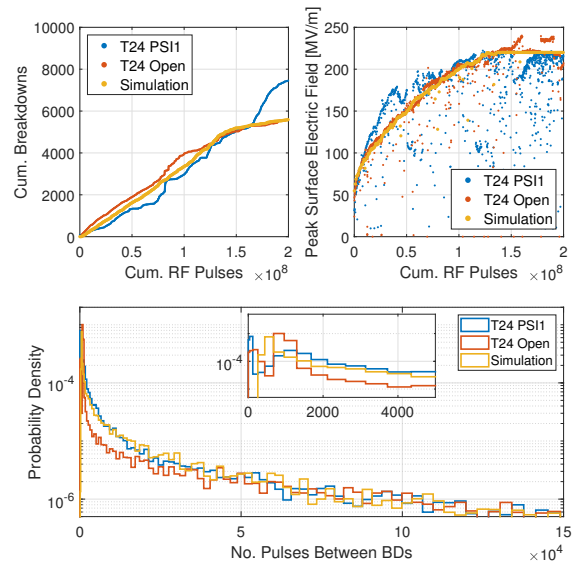
Figure 1: The peak surface electric field (top left), breakdown accumulation (top right), and a probability distribution of the number of pulses between breakdowns for all grid elements (bottom). The results of two prototype high-gradient cavity tests are also shown for comparison.

The resulting conditioning curves resemble those of existing structures. Previously, the distribution of the number of pulses between breakdowns has been described as the sum of two exponential terms [8, 20] however in this case, the probabilistic behaviour of breakdowns has been replicated using only a standard Gaussian distribution acting on numerous, independent elements. Due to the high power employed in Eq. (5), the probability of breakdown is sensitive to changes in the denominator. A consequence of this approach is that the assigned ψ values do not remain centered on the mean due to higher, more stable values being favoured. The minimum and maximum final ψ values were 1.12 and 1.4 respectively, while the average was 1.29.

In CERN's test stands, pulsing is inhibited for several seconds following a breakdown and the field is then automatically ramped back up to the previously achieved level. The discrepancy present from 0-2000 pulses in the probability distribution in Fig. 1 can then be explained by changes in the control system between tests i.e. how quickly the field level was re-established following breakdowns.

Spatially Resolved Conditioning

A variation in the surface field distribution is typical in RF cavities. Consequently, breakdown sites are often distributed

inhomogenuously and visual inspections have shown that they predominantly occur where the surface electric field is highest [10, 24]. This effect was particularly prominent in the test of the CLIC crab cavity, where the electric and magnetic fields are maximised at different angular positions [24]. Following the high-power test, the cavity was cut open via wire electrical discharge machining and the breakdown sites were counted [25]. The surface electric field and breakdown distribution are shown for a single cell in Fig. 2.
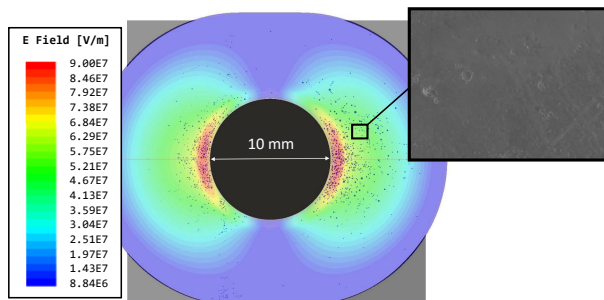
Figure 2: Electric field distribution of cell 2, iris 2 of the CLIC crab cavity with the breakdown locations superimposed. An SEM image of the breakdown sites is also shown.

The clear spatial variation in the surface electric field and breakdown distribution make this result well suited to benchmarking and investigative studies. A portion of a crab cavity cell was meshed with a total of 1350 elements ranging in area from $0.0793 \, \text{mm}^2$ on the peak field regions, to $0.3396 \, \text{mm}^2$ on the cell perimeter where little activity is expected. As the simulated portion constitutes only one fortieth of the total cavity, P_{Ref} and the breakdown rate setpoint were reduced to 1.25×10^{-6} and 7.5×10^{-7} bpp respectively. To provide the correct probabilistic behaviour, the standard deviation of the Gaussian distribution from which the ψ values are taken was set to 0.2. In simulation, the peak surface electric field was ramped up to 220 MV/m and held constant for 50 million pulses. The results are shown in Fig. 3.

The regions where the electric field is highest accrue the majority of the breakdowns, and the angular distribution resembles that of the real cavity. Due to the variation in surface field, different regions are conditioned to different field levels and the model predicts that the ratio between the operating field and the field level to which the surface is conditioned is consistently higher in the peak field regions during operation. Consequently, if the strong empirical scaling in Eq. (2) applies to a cavities global behaviour, it would not be adhered to locally on the surface where there is a variation in the applied field. This result suggests that peak field regions then limit the rate at which the voltage is increased during conditioning, effectively regulating the process.

CONCLUSIONS

A discretised model has been developed and, while relying on several assumptions, offers potential explanations for several experimentally observed phenomena. Notably,
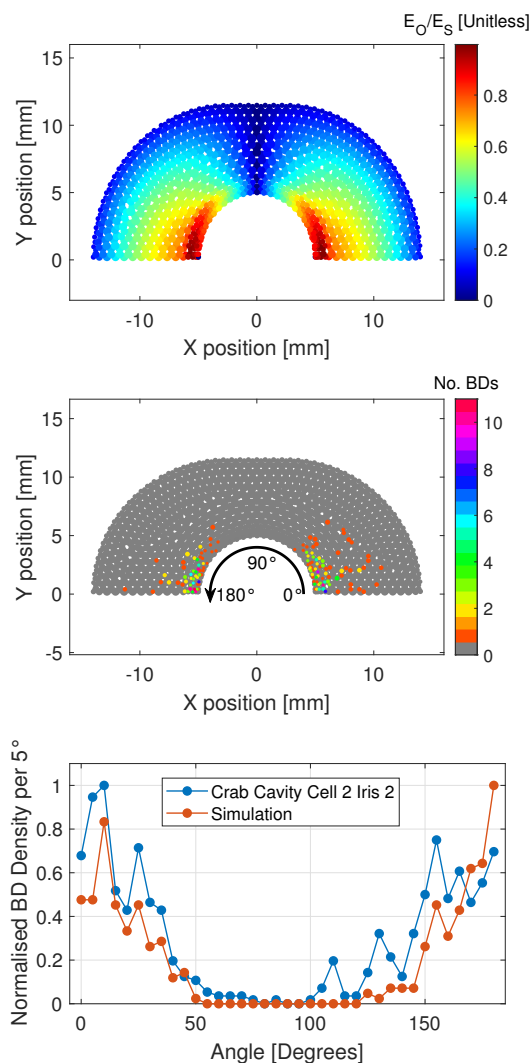
Figure 3: Simulation results for one quarter of a CLIC crab cavity cell showing the elements' final E_O to E_S ratios (top), the number of breakdowns they accrued (centre), and the number of breakdowns per 5° slice normalised to the maximum. Experimental data is plotted with the latter for comparison.

the model reproduces the probabilistic behaviour and inhomogenuous distribution of vacuum arcs well, using only a standard Gaussian distribution acting on independent mesh elements. The current model is defined in terms of the surface electric field, however the use of other quantities such as the modified Poynting vector [13], the breakdown-loaded electric field [26], or a combination thereof, can easily be implemented. Similarly, the use of alternative probability distributions is another aspect which can be investigated with the framework.

REFERENCES

[1] B. Woolley, "High power X-band RF test stand development and high power testing of the CLIC crab cavity", Ph.D. thesis, Lancaster University, Lancaster, 2015.

[2] S. Matsumoto *et al.*, "Nextef: The 100MW X-band Test Facility in KEK", in *Proc. EPAC'08*, Genoa, Italy, Jun. 2008, paper WEPP096, pp. 2740–2742.

[3] M. M. Peng *et al.*, "Development of Tsinghua X-Band High Power Test Facility", in *Proc. IPAC'18*, Vancouver, Canada, Apr.-May 2018, pp. 3999–4001. doi:10.18429/JACoW-IPAC2018-THPAL150

[4] N. Catalan-Lasheras *et al.*, "Commissioning of XBox-3: A Very High Capacity X-band Test Stand", in *Proc. LINAC'16*, East Lansing, MI, USA, Sep. 2016, pp. 568–571. doi:10.18429/JACoW-LINAC2016-TUPLR047

[5] A. Vnuchenko *et al.*, "Design and Construction of a High-Gradient RF Lab at IFIC-Valencia", in *Proc. IPAC'17*, Copenhagen, Denmark, May 2017, pp. 4272–4275. doi:10.18429/JACoW-IPAC2017-THPIK081

[6] S. Pioli *et al.*, "TEX - an X-Band Test Facility at INFN-LNF", in *Proc. IPAC'21*, Campinas, Brazil, May 2021, pp. 3406–3409. doi:10.18429/JACoW-IPAC2021-WEPAB314

[7] H. T. C. Kaufmann, I. Profatilova, I. Popov, W. Wuensch, and M. S. Benilov, "Investigation of Vacuum Breakdown in Pulsed DC Systems", *29th International Symposium on Discharges and Electrical Insulation in Vacuum*, 2012, pp. 19–22. doi:10.1109/ISDEIV46977.2021.9587237

[8] J. G. Navarro, "Breakdown studies for high gradient RF warm technology in: CLIC and hadrontherapy linacs", Ph.D thesis, Universitat de València, Valencia, 2016.

[9] A. Degiovanni, W. Wuensch, and J. Giner Navarro, "Comparison of the conditioning of high gradient accelerating structures", *Phys. Rev. Accel. Beams*, vol. 19, Iss. 3, p. 032001, Mar. 2016. doi:10.1103/PhysRevAccelBeams.19.032001

[10] T. Lucas, "High Field Phenomenology in Linear Accelerators for the Compact Linear Collider", Ph.D thesis, University of Melbourne, Melbourne, 2018.

[11] N. Catalan-Lasheras *et al.*, "High Power Conditioning of X-Band RF Components", in *Proc. IPAC'18*, Vancouver, Canada, Apr.-May 2018, pp. 2545–2548. doi:10.18429/JACoW-IPAC2018-WEPMF074

[12] W. Wuensch *et al.*, "A Demonstration of High-Gradient Acceleration", in *Proc. PAC'03*, Portland, OR, USA, May 2003, paper ROAA011, pp. 495–497

[13] A. Grudiev, S. Calatroni, and W. Wuensch, "New local field quantity describing the high gradient limit of accelerating structures", *Phys. Rev. ST Accel. Beams*, vol. 12, p. 102001, Oct. 2009. doi:10.1103/PhysRevSTAB.12.102001

[14] Y. I. Levinsen, S. Calatroni, A. Descoeudres, M. Taborelli, and W. Wuensch, "Statistical Modeling of DC Sparks", in *Proc. PAC'09*, Vancouver, Canada, May 2009, paper TU5PFP012, pp. 833–835.

[15] A. Grudiev and W. Wuensch, "Design of the CLIC Main Linac Accelerating Structure for CLIC Conceptual Design Report", in *Proc. LINAC'10*, Tsukuba, Japan, Sep. 2010, paper MOP068, pp. 211–213.

[16] A. Grudiev, W. Wuensch, "Design of an X-Band Accelerating Structure for the CLIC Main Linac", CERN, Geneva, Rep. CERN-OPEN-2009-016. CLIC-Note-773, Oct. 2008.

[17] M. Aicheler, *et al.*, "A Multi-TeV Linear Collider Based on CLIC Technology:CLIC Conceptual Design Report", CERN, Geneva, Rep. CERN-2012-007, 2012.

[18] T. G. Lucas, *et al.*, "High power testing of a prototype CLIC structure: TD26CC R05 N3", CERN, Geneva, Rep. CERN-ACC-2018-0030. CLIC-Note-1080, Sep 2018.

[19] R. Zennaro *et al.*, "High Power Tests of a Prototype X-Band Accelerating Structure for CLIC", in *Proc. IPAC'17*, Copenhagen, Denmark, May 2017, pp. 4318–4320. doi:10.18429/JACoW-IPAC2017-THPIK097

[20] W. Wuensch, *et al.*, "Statistics of vacuum breakdown in the high-gradient and low-rate regime", *Phys. Rev. Accel. Beams*, vol. 20, no. 1, p. 011007, 2017.

[21] K. N. Sjobak, A. Grudiev, and E. Adli, "New Criterion for Shape Optimization of Normal-Conducting Accelerator Cells for High-Gradient Applications", in *Proc. LINAC'14*, Geneva, Switzerland, Aug.-Sep. 2014, paper MOPP028, pp. 114–116.

[22] P. Burrows *et al.*, "The Compact Linear Collider (CLIC) - 2018 Summary Report", CERN, Geneva, Rep. CERN-2018-005-M, Dec. 2018. https://doi.org/10.48550/arXiv.1812.06018

[23] W. L. Millar, "Operation of Multiple Accelerating Structures in an X-Band High-Gradient Test Stand", Ph.D thesis, Lancaster University, Lancaster, 2021.

[24] B. Woolley, *et al.*, "High-gradient behavior of a dipole-mode rf structure", *Phys. Rev. Accel. Beams*, vol. 23, p. 122002, Dec. 2020. doi:10.1103/PhysRevAccelBeams.23.122002

[25] E. R. Castro, "Post-Mortem analysis of CLIC Crab Cavity", *International Workshop on Breakdown Science and High Gradient Accelerator Technology*, 2016.

[26] J. Paszkiewicz, "Studies of Breakdown and Pre-Breakdown Phenomena in High Gradient Accelerating Structures", Ph.D thesis, University of Oxford, Oxford, 2020.